

Medical Image Segmentation of Blood Vessels Based on Clifford Algebra and Voronoi Diagram

Zhen Jie Huang, Guo Heng Huang*, Liang Lun Cheng

College of Automation, Guangdong University of Technology, Guangzhou510006, Guangdong, China.

*Corresponding author. Tel: +86 13560231128; email: kevinwongdh@126.com

Manuscript submitted May 21, 2018; accepted June 5, 2018.

doi: 10.17706/jsw.13.6.360-373

Abstract: First, a region growing algorithm based on Clifford algebra is put forward to segment blood vessels of abdominal aorta. Compared with the traditional region growing method, the proposed algorithm is easy to operate and good at robustness. Furthermore, it is available to segment both normal and abnormal blood vessels of abdominal aorta: the seed point can keep on growing even when there are some isolated points in region of blood vessels. The key point of this algorithm is that: the gray values of eight neighborhood points are composed as unit feature vectors of current seed points, and then Clifford algebra vector product representation will be applied. Second, for the purpose to segment thinner global abdominal blood vessels rapidly, a novel segmentation algorithm of blood vessels based on 2D Voronoi diagram is put forward as an attempt. Experiments demonstrate that it is potential to segment thinner global abdominal blood vessels fast. In the future, this algorithm is potential to segment blood vessels in abdominal organs.

Key words: Medical image segmentation, blood vessels, Clifford algebra, Voronoi diagram

1. Introduction

Recently, virtual surgeon simulation becomes more and more important to assist surgeon and perform better therapy treatment. Research on virtual surgeon simulation generally includes extraction for the Region of Interest (ROI), 3D reconstruction for medical images; surgeon simulation and so on. Therein, for the purpose to reduce the amount of data and locate lesions, extracting the ROI is very important, such as blood vessels, tumors and other organs segmentation. There are many methods applied to segment vessels from different human organs. Segmentation of vessels mainly includes segmentation for liver vessels, retinal vessels and cholic vessels etc. Many methods were proposed into this field to segment vessels of different organs. Therein, an algorithm based on a NN scheme for voxel classification was applied to segment retinal vessels [1]. However, it could only be applied to 2D images but 3D image series. Esneault et al. proposed a fast and fully automatic method based on geometric moments and Graph Cut technique to segment liver vessels [2]. However, this algorithm was not effective to segment thinner vessels and sensitive to interpolation of image slices. Bashar et al. put forward a component-based structural measure named "Hole Area Index (HAI)" to isolate bone, soft-tissue structures and segment thinner and larger vessels [3]. However, pre-enhancement was necessary to incorporate some missing thinner vessels, and these enhancements also enhanced undesired structures. Moreover, level set theory is one of the most popular methods which are applied to vessels segmentation. Therein, Hong et al. put forward local binary fitting energy in the hybrid level set method to extract local information on MRA image more accurately, and it could also be applied on

CT image [4]. Although it could solve the problem that traditional hybrid level set could not produce a satisfactory segmentation for medical images with high intensity homogeneity, it was only a solution to segment thinner vessels. So far, none of the above solutions could be successful to segment vessels on low contrast and heterogeneous environments, especially for eliminating bones around larger vessels.

To our best knowledge, there are few methods so far which are applied for the global abdominal vessel extraction without the bones around vessels [3]. It is difficult to segment vessels without bones. Therefore, we propose two novel algorithms to segment abdominal vessel. On one hand, 3D region growing algorithm based on Clifford algebra vector product representation is put forward to segment the blood vessels for abdominal aorta; on the other hand, for the purpose to segment thinner global abdominal vessel without major bones and organs, another novel blood vessel segmentation algorithm based on 2D Voronoi diagram is also put forward as an attempt.

2. Related Works

2.1. Clifford Algebra

Let (e_0, e_1, \dots, e_n) be an orthogonal basis in the linear space over R [5], the Clifford algebra A_n is an associative algebra which is composed by (e_0, e_1, \dots, e_n) , then $e_0^2 = e_0, e_i e_0 = e_0 e_i = e_i, e_i^2 = -1, i = 1, 2, \dots, n$. $e_i e_j = -e_j e_i, 1 \leq i \neq j \leq n$.

Elements in A^n are known as the Clifford algebra, $\forall x \in A^n, x$ have the form that $x = \lambda_0 + \sum \lambda_A e_A, A = A = (h_1, \dots, h_p), 1 \leq h_1 < \dots < h_p \leq n, 1 \leq p \leq n, e_A = e_{h_1} e_{h_2} \dots e_{h_p}, \lambda_A \in R$. Obviously, A^n is $2n$ -dimensional associative and non-commutative algebra. If Clifford algebra x has the form $\underline{x} = x_0 + \sum_{i=1}^n x_i e_i, x$ is called as Clifford vector. For $\forall x \in A^n$, Clifford mold of x is defined as $|x| = 2^{\frac{n}{2}} (\sum \lambda_A^2)^{\frac{1}{2}}$. Especially, the mold of Clifford vector x is $|\underline{x}| = 2^{\frac{1}{2}} (\sum_{i=1}^n x_i^2)^{\frac{1}{2}}$.

If $\underline{x} = \sum_{i=1}^n x_i e_i$ and $\underline{y} = \sum_{i=1}^n y_i e_i$ are two unit Clifford vector, in accordance with the rule of Clifford algebra multiplication,

$$\underline{x} \underline{y} = (\sum_{i=1}^n x_i e_i) (\sum_{i=1}^n y_i e_i) = -\sum_{i=1}^n x_i y_i + \sum_{1 \leq i, j \leq n} (x_i y_j - x_j y_i) e_i e_j \tag{1}$$

Under normal circumstances, the product of two n -dimensional Clifford vector is no longer an n -dimensional Clifford vector. In other words, the Clifford vector by the n -dimensional linear subspace Clifford multiplication is not closed. $x \times y$ is denoted by $\sum_{1 \leq i, j \leq n} (x_i y_j - x_j y_i) e_i e_j$, and it is defined as the outer product of x and y .

Theorem Suppose that q_1 and q_2 are pure unit Clifford algebra, and the components of q_1 and q_2 are all non-negative. Then $q_1 = q_2 \Leftrightarrow q_1 q_2 = -q_1 \times q_2 = -1$.

2.2. Dimension Voronoi Digram

Dirichlet and Voronoi firstly introduced this concept. This concept was used to research the quadratic form: let quadratic matrix of data be as a node, and the scope of node was reflected by the Euclidean norm. Later, this concept was known as Voronoi diagram [6]-[9].

Voronoi firstly studied this structure on the dual nature which was mentioned by Descartes. He connected all adjacent nodes through lines, and got a triangular mesh finally. Subsequently, Delaunay studied the triangulation of two-dimensional point set and obtained the same triangular mesh. Then Delaunay studied

two-dimensional point set triangulation and obtained the same triangular mesh what Voronoi got before. Each edge of this triangle mesh was strictly limited what was given by Delaunay: there is a circle that goes pass the edge of two endpoints, and this circle does not contain the other point. Voronoi and Delaunay's results proved the dual graph found by Voronoi was the triangular mesh constructed by Delaunay. Thereupon, the dual graph of Voronoi diagram was also named as Delaunay triangulation.

The principle of 2D Voronoi diagram classification is that [10]: classify the pending processed area in image by using 2D, and iterate until find out the boundary of the image. In the case of 2D plane, plane is divided into several areas refer to n discrete points of plane. Therein, there a discrete point in each area which is a set that most nearly to the point. It is defined as:

For $\forall p_i \in V$, $V = \{p_1, p_2, \dots, p_n\}$, then $Vor(p_i) = \{x \in R^2 \mid d(x, p_i) \leq d(x, p_j), \forall j \neq i, 1 \leq j \leq n\}$. Therein, $d(p, x) = \sqrt{(p_1 - x_1)^2 + (p_2 - x_2)^2}$ is the Euclidean distance between $p = (p_1, p_2)$ and $x = (x_1, x_2)$.

Besides, Delaunay triangulation and Voronoi diagram is duality. There is a corresponding Delaunay triangulation to each given 2D Voronoi diagram. The specific relationship is as follows: in 2D plane, the Voronoi vertex of each 2D Voronoi diagram corresponds to a triangle in the Delaunay triangulation, and this vertex is the circumcenter of the triangle in the Delaunay triangulation; each edge in the 2D Voronoi diagram corresponds to one edge in the Delaunay triangulation, and they will be vertical; each sub-structure for 2D Voronoi diagram corresponds to a vertex in the Delaunay triangulation, and this vertex is the Delaunay triangulation which corresponds to the vertex of the sub-structure of Voronoi diagram.

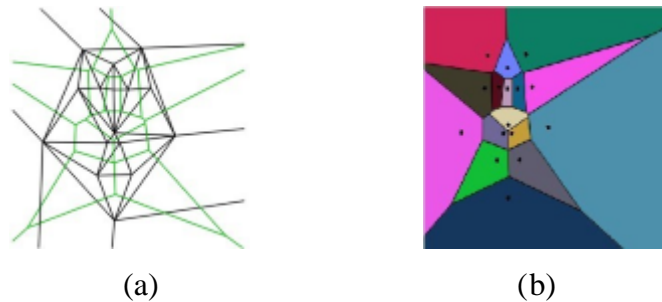


Fig. 1. 2D Voronoi diagram: (a) Delaunay triangulation of 16 points; (b) corresponding Voronoi division.

In addition, for image processing, the vertices of the 2D Voronoi diagram are the "skeleton" of a closed connected region in the image plane. At present, algorithms based on 2D Voronoi diagram even 3D Voronoi diagram have been applied in the field of image segmentation, fluid simulation and so on.

3. Algorithms

3.1. Region Growing Based on Clifford Algebra

In order to go on growing in the blood vessels areas with isolated voxels when we segment the blood vessels, a novel Region Growing algorithm based on Clifford algebra is put forward to segment more blood vessels of abdominal aorta. In accordance with Clifford algebra vector product representation theorem which was mentioned at the previous section, if two unit vectors are equal when and only when their inner product value is 1; if two unit vectors are similar, their inner product will be closer to 1. In 3D data of CT image series, if two adjacent voxels are the same or similar, the inner product between the eight-dimensional feature vectors composed by the gray values of their eight neighborhoods should be equal to 1 or near to 1. Sum up, the procedure of Region Growing algorithm based on Clifford algebra is:

Step 1, input k pieces of $m \times n$ contiguous CT series images (3D volume data, size is $m \times n \times k$), and select the initial seed points in target areas.

Step 2, calculate the gray values of eight neighborhoods of current seed point, and they will compose an eight-dimensional vector and be unitized. Then the eight-dimensional unit vector is defined as the eight-dimensional unit feature vector of current seed point, it represents the feature of current seed point. The definition of eight neighborhoods in Region Growing algorithm based on Clifford algebra is as Fig. 2.

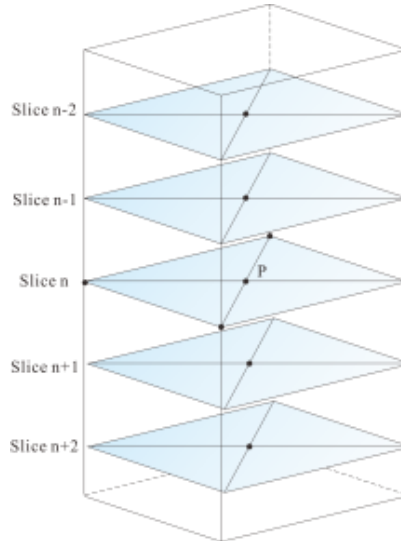


Fig. 2. The definition of eight neighborhoods of Region Growing based on Clifford algebra.

Step 3, calculate the unit eight-dimensional feature vectors of six neighborhoods of current seed points, and find the neighborhoods whose inner products of feature vector with current seed point within a given interval which is close to 1 (in this paper, the given interval is $[0.995, 1]$). Then these neighborhoods will be incorporated into the current voxel region of seed point, and become a new seed point. Iterate is over when neighborhood which fulfills the rule cannot be found again. The workflow chart of this algorithm is as Fig. 3.

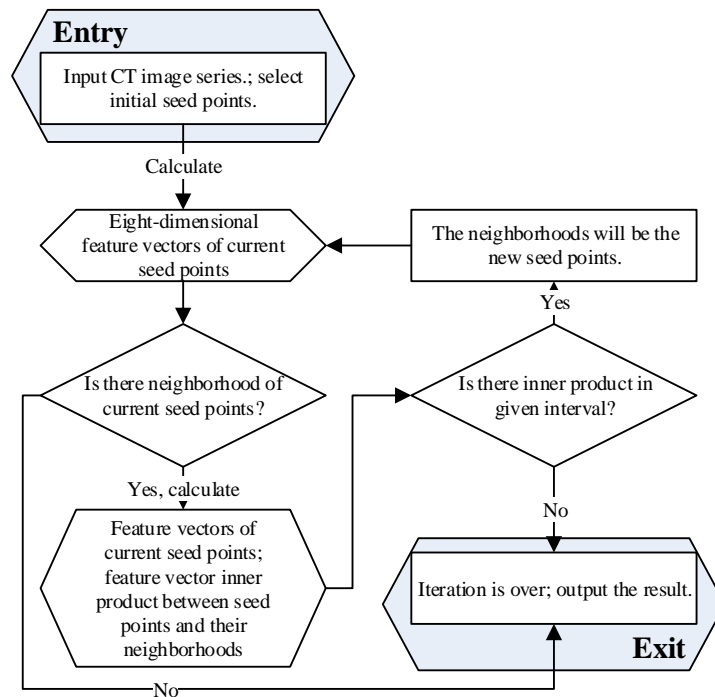


Fig. 3. The flow chart of region growing based on Clifford algebra.

Different from traditional Region Growing algorithms which just consider the gray value of the current points, Region Growing algorithm based on Clifford algebra fully considers the feature of neighborhoods of current points.

3.2. Vessel Segmentation based on 2D Voronoi Diagram

It has been lacking a feasible way to segment the global thinner abdominal blood vessels (thinner blood vessels are defined as non-aortic vessels whose size are less than or equal to the size of the third layer of abdominal aorta). In addition, the segmentation of thinner non-aortic abdominal blood vessels is very important to surgeon of pancreas, spleen and other abdominal organs. In CT series, it includes three main types of the thinner abdominal blood vessels: horizontal vessels, diagonal vessels and vertical vessels. The thinner horizontal blood vessels would be rough thin lines in each CT slice; the thinner vertical blood vessels would be thin points in pre CT slice; the thinner diagonal blood vessels would be regarded as the combination of thin lines and thin points in each CT slice. Therefore, at the premise of being denoised, if thin lines and points in each slice can be segmented that means it is possible to segment the thinner abdominal blood vessels.

Combined with the Voronoi diagram theory which was mentioned previously, a novel segmentation algorithm of blood vessels based on 2D Voronoi diagram is designed specifically for segmentation of the global thinner abdominal blood vessels. The whole procedure will be:

Step 1, import the original CT series one by one, and then Threshold segmentation is applied as pre-segmentation, the remaining are all organs, blood vessels and bones. Then, import the original CT series one by one again, and then traditional Region Growing is applied to segment abdominal aorta. Finally, subtract the results of Threshold segmentation and Region Growing. The remaining will be voxels of bones, organs and thinner abdominal blood vessels.

Step 2, consider the edge voxels as sampling points, and then input them as the initial vertices of algorithm based on two-dimensional Voronoi diagram. Then, execute this algorithm and the output result is the set of Voronoi vertices. For each closed interval (inner vessels region), there exist a central axis which connect to the vertices of each Voronoi diagram, and it can be seen as "skeleton" of two-dimensional blood vessel images. It is possible that a sampling point is the intersection of enclosed areas, so it may correspond to more than one axis. Define the set of central axis which corresponds to sampling point P as \mathcal{Q} , and then define the size of two-dimensional image by using the shortest distance from P to \mathcal{Q} .

Step 3, set the threshold radius, and the sampling whose distance to central axis does not exceed the threshold will be retained. During actual operation, the density of sampling points is high, so the sampling point to the distance corresponding to two-dimensional Voronoi vertex set can be approximated as the distance between the sampling point and the central axis set. When the distance does not exceed the radius is to keep the sampling points. After this operation, the sampling point set is expressed as R .

Step 4, calculate the Delaunay triangulation of R . The triangulation impacts inside and outside of the enclosed region. As the result of an enclosed area inside is needed, it is necessary to remove the external triangle region. Through observation, the triangles in the triangulation of outside region, the shape mostly is the slender-shaped obtuse triangle; however, more acute triangle is inside the enclosed region, even if there is an obtuse triangle, its circumcircle radius must not exceed the radius. Therefore, to calculate the radius of all the circumcircle of the triangle, Threshold filtering, it can remove the triangular area outside the enclosed area, and results of the entire algorithms are obtained finally.

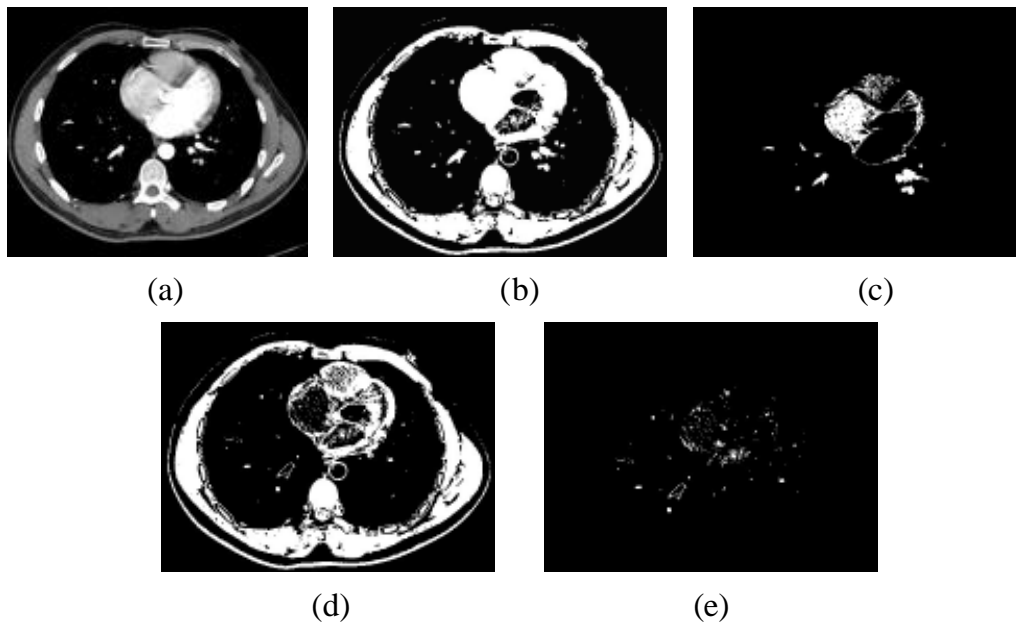


Fig. 4. The whole process of segmentation algorithm based on 2D Voronoi diagram: (a) original image; (b) initial result of traditional threshold segmentation; (c) result of traditional region growing; (d) subtracting result between results of threshold segmentation and region growing; (e) the final result of the proposed segmentation algorithm based on 2D Voronoi diagram.

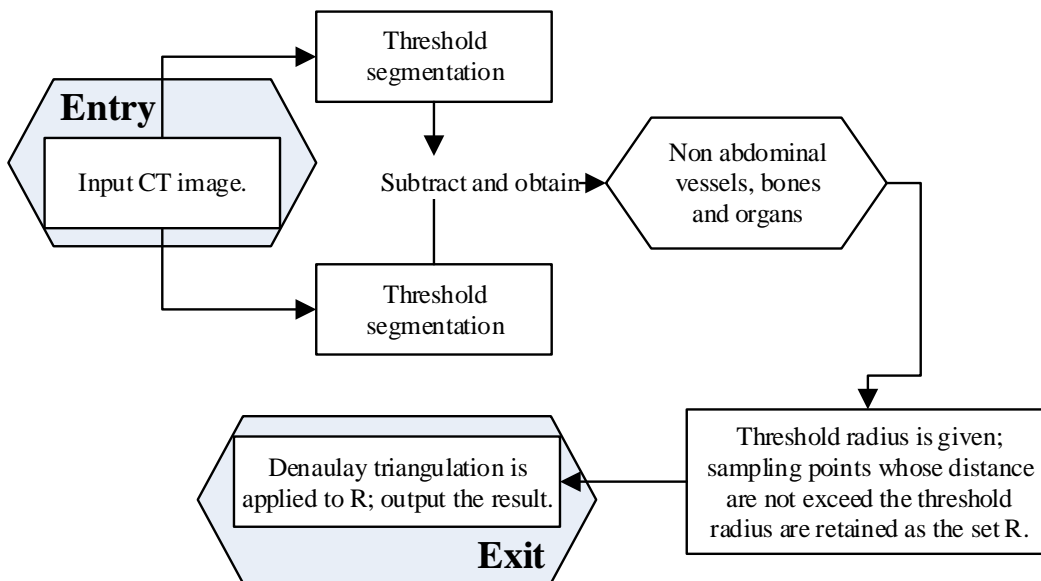


Fig. 5. The flow chart of Vessel Segmentation based on Voronoi diagram.

In addition, because of the complexity of the enclosed area (several small holes in the internal of large area), Denaulay triangulation made mistakes on segmenting part of the background. To solve this problem, sample the voxels inside the triangle by the color information to determine whether it belongs to the foreground. In engineering, bitwise operations are applied to combine with the filling after Delaunay triangulation with the original image.

4. Experimental Results

All experiments will be performed in Microsoft Windows7. In this thesis, all experimental data for

Abdominal CT images were provided by the Pearl River Hospital from Southern Medical University, and the size of each slice of images is 512×512. The experimental environment is: CPU is Intel Core i7-3517U 1.90GHz CPU, and RAM is 4GB.

4.1. Region Growing Based on Clifford Algebra

Segment S50 (365 slices) and S70 (320 slices) these two sets of data with abdominal aorta respectively by region growing based on confident interval and Clifford algebra, and compare the results.

First, segment the abdominal aorta for S50 and S70 by the two algorithms, and then select four initial seed points. The initial seed points is distributed as Fig. 6.

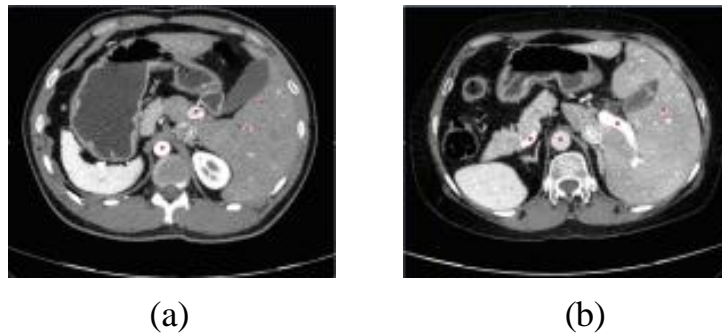


Fig. 6. The distribution of initial seed points on S50 and S70: (a) the initial seed points on slice 183rd of S50; (b) the initial seed points on slice 161st of S70.

The segmentation results for abdominal aorta from S50 by using traditional region growing based on confident interval and the proposed segmentation algorithm based Clifford algebra are shown by Fig. 7.

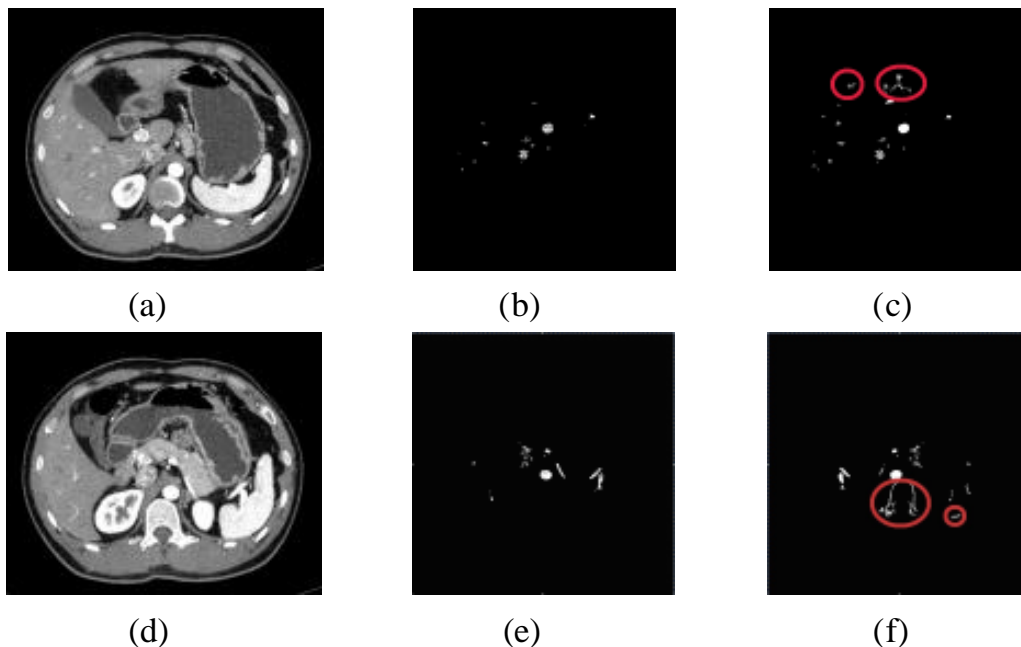


Fig. 7. The segmentation result of abdominal aorta from two algorithms on S50: (a) & (d) the original images on slice 182nd and 205th; (b) & (e) results from region growing based on confident interval; (c) & (f) results from the proposed method based on Clifford algebra.

The segmentation results for abdominal aorta from S70 by using region growing based on Confident interval and Clifford algebra are shown by Fig. 8.

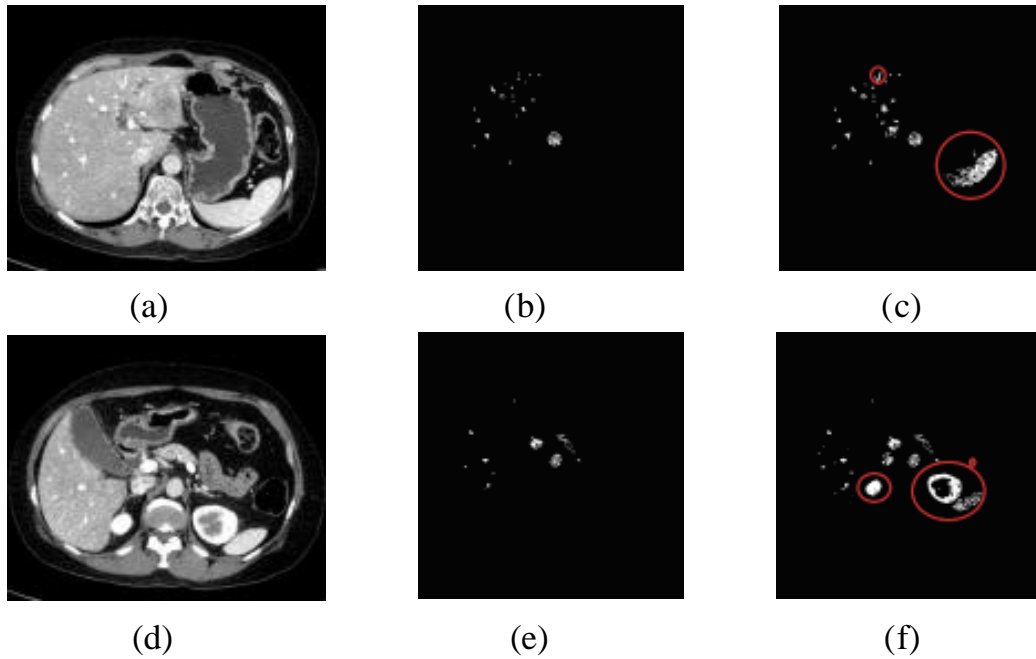


Fig. 8. The segmentation result of abdominal aorta from three algorithms on S70: (a) & (d) the original images on slice 109th and 199th; (b) & (e) results from region growing based on confident interval; (c) & (f) results from the proposed method based on Clifford algebra.

The 3D reconstruction results on S50 and S70 which are obtained after Region Growing algorithms based on Confident interval and Clifford algebra are shown respectively by Fig. 9 and 10.



Fig. 9. The 3D reconstruction results of two algorithms on S50: (a) result from region growing based on confident interval; (b) result from the proposed method based on Clifford algebra.



Fig. 10. The 3D reconstruction results of two algorithms on S70: (a) result from region growing based on confident interval; (b) result from the proposed method based on Clifford algebra.

Then, abdominal non-aorta from S50 with only one initial seed point will be segmented by traditional Region Growing, Region Growing based on Confident interval and Clifford algebra. The initial seed point and results of segmentation are shown by Fig. 11.

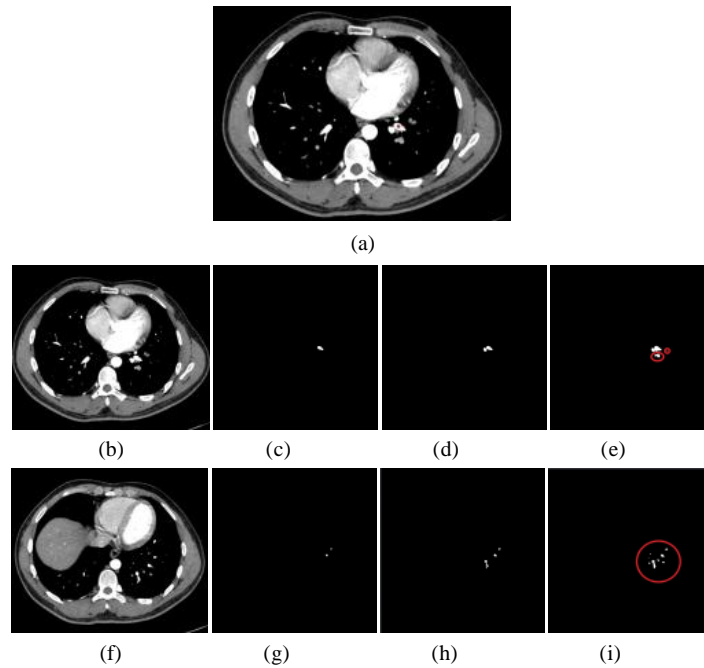


Fig. 11. Visual comparison on S50: (a) seed point of S50, slice 1st; (b) & (f) the original images; (c) & (g) results from traditional region growing; (d) & (h) results from region growing based on confident interval; (e) & (i) results from the proposed method based on Clifford algebra.

The 3D reconstruction results on abdominal non-aorta from S50 which are extracted after Region Growing algorithms based on Confident interval and Clifford algebra are shown by Fig. 12.

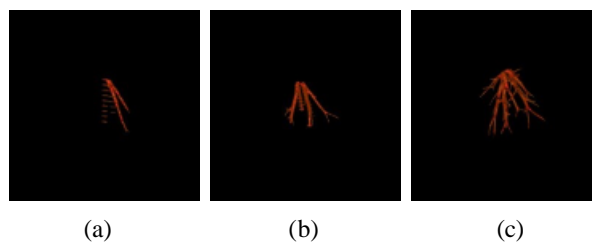


Fig. 12. The 3D reconstruction result of three algorithms: (a) result from traditional region growing; (b) result from region growing based on confident interval; (c) result from the proposed method based on Clifford algebra.

Afterwards, performance analysis of segmentation of Region Growing algorithm based on traditional Confident interval and Clifford algebra on S50 (365 slices, four seed points), S70 (320 slices, four seed points) and S50 (one seed point) will be shown as the below tables.

Table 1. Segmentation Summary for S50 Part1

Method	Runtime	Analysis
Confident interval	136.92s	Fewer vessels were segmented; bones and organs were not segmented.
Clifford algebra	728.55s	More vessels were segmented; bones and organs were segmented.

Table 2. Segmentation Summary for S50 Part2

Method	Runtime	Analysis
Region growing	68.34s	Fewest vessels were segmented.
Confident interval	99.02s	Fewer vessels were segmented.
Clifford algebra	466.85s	Most vessels were segmented.

Table 3. Segmentation Summary for S70

Method	Runtime	Analysis
Confident interval	117.34s	Fewer vessels were segmented.
Clifford algebra	594.07s	More vessels were segmented, but part of liver was segmented.

3D region growing algorithm based on Clifford algebra vector product representation are proposed by this paper, and experimental performance data can be seen from the above tables: when traditional Region Growing algorithm and Region Growing algorithm based on Confidence interval are applied to segmented abdominal aorta, if it grows to the isolated voxels between the regions of vessels, it may not keep on growing. However, it is not only that the current voxels' gray values are considered by 3D region growing algorithms based on Clifford algebra, but also the neighborhoods of the current voxels are considered. Therefore, on one hand, if there is only one breakpoint in the vessel regions, the seed points can continue to grow and segment the blood vessels by these two methods; on the other hand, comparing with algorithm based on Clifford algebra, though more layers of abdominal aorta are segmented by the algorithm based on Clifford algebra than traditional Region Growing, some of non-interesting regions were be extracted such as other organs or bones. The reason is too many neighborhoods are considered to compose a feature vector of the seed points to blur the differences between points. Then seed points would grow to non-interesting regions of different qualities.

4.2. Vessel Segmentation Based on 2D Voronoi Diagram

Compared with traditional Threshold segmentation, blood segmentation algorithm based on 2D Voronoi diagram is applied to segment thinner abdominal blood vessels from first 80 slices of S50 and S70. The segmentation results are shown by Fig. 13 and 14.

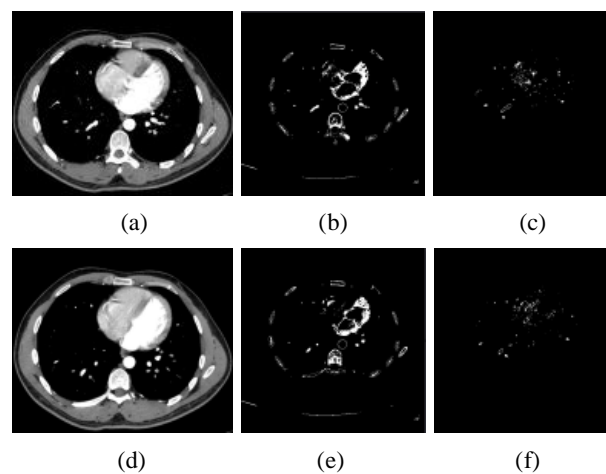


Fig. 13. The segmentation results of S50 in its first 80 slices: (a) & (d) the original images; (b) & (e) results from traditional threshold segmentation; (c) & (f) results from the proposed segmentation based on 2D Voronoi diagram.

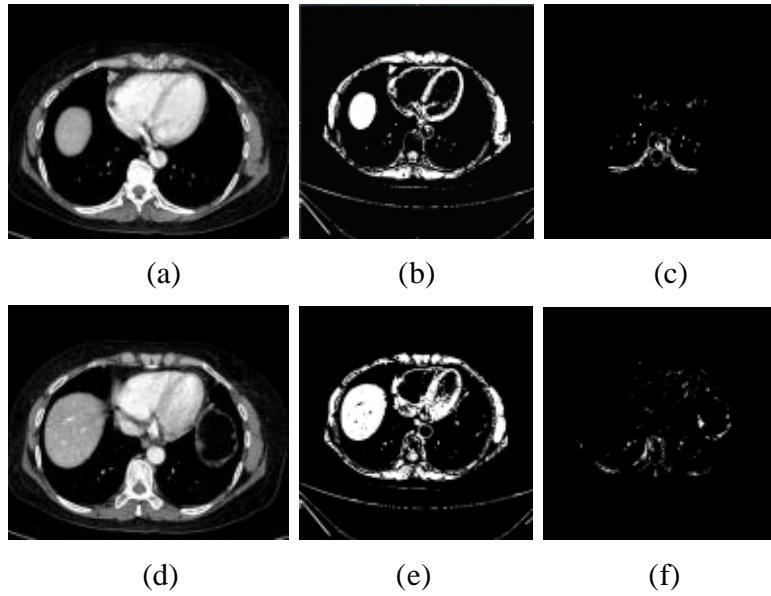


Fig. 14. The segmentation results of S70 in its first 80 slices: (a) & (d) the original images; (b) & (e) results from traditional threshold segmentation; (c) & (f) results from the proposed segmentation based on 2D Voronoi diagram.

The 3D reconstruction of the segmentation results of these algorithms are shown by Fig. 15 and 16.

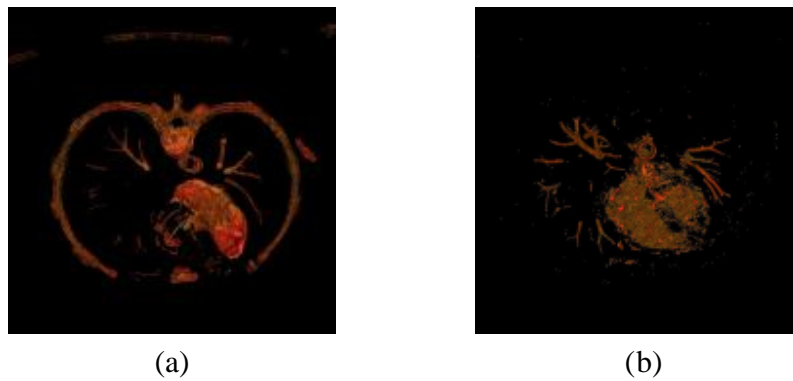


Fig. 15. The reconstruction of thinner blood vessels of abdominal non-aorta on the first 80 slices of S50.

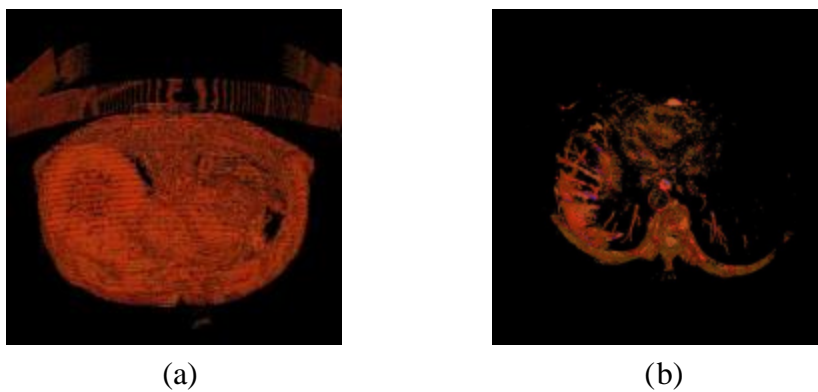


Fig. 16. The reconstruction of thinner blood vessels of abdominal non-aorta on the first 80 slices of S70.

It can be seen from two previous figures: on one hand, more of thinner blood vessels of abdominal

non-aorta excluding mostly bones and soft tissue by algorithm based on 2D Voronoi diagram, but there will be more discrete points in the segmentation results; on the other hand, Threshold segmentation may not only segment fewer thin blood vessels, but also non-interested organs. Compared with the 3D Region Growing algorithm based on Clifford algebra, poorer segmentation results are got by algorithm based on 2D Voronoi diagram. It needs to select many initial seed points to segment the global vessels that may waste a lot of time to compute. However, the thinner blood vessels of abdominal non-aorta can be segmented rapidly by algorithm based on 2D Voronoi diagram. This method is potential to be applied in clinical practice.

Table 4. Segmentation Summary for S50

Method	Runtime	Analysis
Threshold	14.25s	Fewer thin vessels were segmented. Organs and bones were segmented. There was not isolated voxel.
2D Voronoi diagram	163.83s	More thin vessels were segmented. Organs and bones were almost not segmented. But there were many isolated voxels.

Table 5. Segmentation Summary for S70

Algorithm	Runtime	Analysis
Threshold	18.94s	Almost no thin vessel was segmented.
2D Voronoi diagram	188.64s	More thin vessels were segmented. Organs and bones were almost not segmented. But there were many isolated voxels.

A novel segmentation algorithm based on 2D Voronoi diagram is proposed to segment more thin blood vessels of abdominal non-aorta excluding the bones and soft tissue. However, there will be many discrete points are segmented by this algorithm. It is due to that this algorithm is a 2D algorithm that considers each slice one by one, but considers the relationship between each slice. However, Voronoi diagram theory has been promoted to 3D, thus blood segmentation algorithm based on 3D Voronoi diagram is potential to solve this problem in the future.

5. Conclusion

Research on the segmentation of the abdominal blood vessels is focused on 3D medical images.

First, existing segmentation methods applied to abdominal aorta segmentation are not good enough. Therefore, a new algorithm based on hypercomplex-3D region growing algorithm based on Clifford algebra is applied to segment abdominal arterial vessels. Compared with traditional region growing, Hessian matrix and genetic algorithm etc., this algorithm is easy to operate and good at robustness. Therefore, it is available to segment both normal and abnormal blood vessels of abdominal aorta: the seed point can go on growing, even when there are some isolated points in region of blood vessels. However, compared with traditional Region Growing algorithms, this algorithm is not fast enough in computing, thus the future work will be focused on algorithm optimization or GPU acceleration.

Second, it has been lacking an algorithm which can segment thinner global abdominal blood vessels rapidly. A novel segmentation algorithm of blood vessels based on 2D Voronoi diagram is put forward as an attempt. Experiments demonstrate that it is valid to segment thinner global abdominal blood vessels by using this algorithm. However, the algorithm is still in the infancy, and has the following shortcomings: first, there are some isolated voxels in the segmentation result. It is all because that segmentation algorithm of blood vessels based on 2D Voronoi diagram is a 2D method, and it does not consider the relationship between the adjacent slices. Second, the segmentation result depends partly on the pre-segmentation result from Threshold and Region Growing. In future work, we will continue to study the blood vessels segmentation algorithm based on 3D Voronoi diagram. The future work will be to consider the relationship between the adjacent slices and remove discrete breakpoints. Besides, this algorithm will also be applied to segment blood vessels in

abdominal organs.

Acknowledgment

This work was sponsored by National Nature Science Foundation of China (grant number 61702111), National Key R&D Plan of China (grant number 2016YFC0800506).

References

- [1] Marin, D., Aquino, A., Gegundez-Arias, M. E., & Bravo, J. M. (2011). A new supervised method for blood vessel segmentation in retinal images by using gray-level and moment invariants-based features. *IEEE Transactions on Medical Imaging*, 30, 146-158.
- [2] Esneault, S., Lafon, C., & Dillenseger, J. L. (2010). Liver vessels segmentation using a hybrid geometrical moments/graph cuts method. *IEEE Transactions on Biomedical Engineering*, 57, 276-283.
- [3] Bashar, M. K., Mori, K., & Kobayashi, T. J. (2010). Automatic segmentation of abdominal blood vessels from contrasted X-ray CT images. *Proceedings of the 2010 International Conference on Electrical and Computer Engineering* (pp. 187-190).
- [4] Hong, Q., Li, Q., & Tian, J. (2010). Local hybrid level-set method for MRA image segmentation. *Proceedings of the 2010 IEEE 10th International Conference on Computer and Information Technology*. (pp. 1397-1402).
- [5] Gong, Y., Leong, I. T., & Qian, T. (2009). Two integral operators in Clifford analysis. *Journal of Mathematical Analysis and Applications*, 354, 435-444.
- [6] Liu, W., & Li, X. A new octonion method for edge detection of color image. Preprinted.
- [7] Okabe, A., Boots, B., & Sugihara, K. (1992). Spatial tessellations: Concepts and applications of Voronoi diagrams: John Wiley & Sons, Inc.
- [8] Aurenhammer, F. (1991). Voronoi diagrams and mdash, a survey of a fundamental geometric data structure. *ACM Comput. Surv.*, 23, 345-405.
- [9] Reem, D. (2009). An algorithm for computing voronoi diagrams of general generators in general normed spaces. presented at the Proceedings of the 2009 Sixth International Symposium on Voronoi Diagrams.
- [10] Voronoi_diagram. Retrieved from http://en.wikipedia.org/wiki/Voronoi_diagram.



Zhenjie Huang was born in Guangdong province, China, in 1993. He graduated in automation from Guangdong University of Technology in 2016. He is a master's student in school of automation of Guangdong University of Technology. His current research is about digital image processing, deep learning and computer vision.



Guoheng Huang was born in Guangdong province, China, in 1985. He received PhD degree in Macau University. He is a lecturer and teaches in Guangdong University of Technology since 2016. His research interests include deep learning, computer vision and machine learning.



Lianglun Cheng was born in Hubei province, China, in 1964, is a Prof. and doctoral supervisor of Faculty of Automation, Guangdong University of Technology. He received PhD degree in Huazhong University of Science and Technology. His current research is about computer vision, image data compression etc.